BEHAVIOR OF AN INERT SCALAR UNDER THE DIFFERENT SMALL SCALE TOPOLOGIES OF A TURBULENT FLOW

César Dopazo, Jesús Martín
Área de Mecánica de Fluidos, Universidad de Zaragoza
María de Luna 8, Zaragoza 50015, Spain

Luis Valiño, Bruno Crespo
LITEC, Consejo Superior de Investigaciones Científicas
María de Luna 3, Zaragoza 50015, Spain

ABSTRACT

The physical phenomena that determine the evolution and characteristics of a scalar in a turbulent flow are studied using direct numerical simulation (DNS) of both the scalar and the velocity fields. The statistics of essential magnitudes related to the mixing, such as the scalar diffusion, the scalar dissipation or the variance is analysed for the different small scale dynamical structures in the flow. This study is conducted in the framework of the Topological Methodology introduced by Chong et al (1990), which classifies the different small scale dynamics in terms of velocity gradient invariants. From this investigation, the scalar properties display different features for each of the four topologies considered.

INTRODUCTION

Scalar mixing in a turbulent flow is a complex process characterized by a wide range of time and length scales, over which a variety of physical mechanisms take place (Ottino, 1989; Dopazo, 1994). The scalar evolution, driven by the turbulent velocity field, involves convection, random straining and rotation, and molecular transport. Scalar heterogeneities are smeared out by molecular diffusion enhanced by stretching and folding of isoscalar surfaces.

The rational formulation of stochastic molecular mixing models crucially depends on the ability to parameterize the scalar mixing mechanisms in terms of the scalar fluctuations, the scalar gradient vector, and knowable information pertaining both to the scalar and to the turbulence fields. It is, thus, logical searching for some correlation of the molecular transport terms in the conservation equations of the scalar related magnitudes and the properties of the velocity field. The statistics of a passive scalar in turbulence has been widely investigated in the past years using DNS (See, for example, Kerr (1985), Ashurst et al (1987); Ruetsch and Maxey (1991) or Pumir (1994), among others). The aim of the present work is to investigate this statistics considering the different patterns or motions that appear in the small scales of a turbulent flow using the topological classification introduced by Chong et al (1990). Specifically, regions in the flow with high kinetic energy dissipation rates (dissipative motions) and regions of high vorticity (focal motions) are of special interest here.

THEORETICAL BACKGROUND

For an inert scalar C the mean value, $< C >$, is a constant and the scalar fluctuations, c, obey the equation (Dopazo, 1994)

$$\frac{\partial c}{\partial t} + u_j \frac{\partial c}{\partial x_j} = D\nabla^2 c. \tag{1}$$

where c is statistically homogeneous, D is the Fickian diffusion coefficient of c in the mixture and $\mathbf{u}$ is a zero-mean statistically homogeneous solenoidal random velocity field.

The transport equation for the scalar gradient fluctuation $c_{,i}$ is

$$\frac{\partial c_{,i}}{\partial t} + u_j \frac{\partial c_{,i}}{\partial x_j} = -c_{,j}\, u_{i,j} + D\nabla^2 c_{,i}\,. \tag{2}$$

The dynamics of the scalar gradient is essential in the scalar field evolution. This vector is perpendicular to the local isoscalar surface, at each point in the flow; the geometry and characteristics of these isosurfaces are determined by the spatial distributions of the scalar gradient vector (Ottino, 1989).

Equation (1) can be alternatively rephrased as

$$\frac{\partial c^2}{\partial t} + u_j \frac{\partial c^2}{\partial x_j} = D\nabla^2 c^2 - 2\epsilon_c. \tag{3}$$

where $\epsilon_c = D c_{,i} c_{,i}$ is the local/instantaneous scalar fluctuation dissipation rate. Apart from the pressure term, the transport equation for c^2 is analogous to that for the instantaneous turbulent kinetic energy.

Ensemble averaging (3) yields

$$\frac{d < c^2 >}{dt} = -2 < \epsilon_c > . \quad (4)$$

which is the equation for the scalar variance decay. The transport equation for the scalar dissipation rate ϵ_c is also readily derived, obtaining

$$\frac{\partial \epsilon_c}{\partial t} + u_j \frac{\partial \epsilon_c}{\partial x_j} = -2Dc_{,i}\, c_{,j}\, u_{j,i} + \\ +D\nabla^2 \epsilon_c - 2D^2 c_{,ij}\, c_{,ij} . \quad (5)$$

The first term on the right hand side of Eq. (5) is the production of ϵ_c by straining of scalar gradients; $u_{j,i}$ may be replaced by its symmetric part S_{ij} and then this term is related to that part of the strain aligned with the local and instantaneous scalar gradient vector, similarly to the production term $S_{ij}\omega_i\omega_j$ in the square-vorticity (enstrophy) equation. The last two terms of (5) are the diffusive transport and dissipation of ϵ_c, respectively.

An adequate tool to characterize the small scale patterns or motions in a turbulent velocity field is the *Topological Methodology* mentioned before. In this approach the turbulent velocity field at each point is characterized by two quantities: R and Q, the second and third invariants of the velocity gradient tensor $A_{ij} = \partial u_i/\partial x_j$. Their expressions for an incompressible flow are

$$Q = -\frac{1}{2} A_{ij} A_{ji} \quad (6)$$

$$R = -\frac{1}{3} A_{ij} A_{jk} A_{ki}. \quad (7)$$

Four different non-degenerate topologies exist in an incompressible flow: Stable focus with stretching (SF/S), unstable focus with contraction (UF/C), unstable node/saddle/saddle (UN/S/S) and stable node/saddle/saddle (SN/S/S). This classification, as given by Chong et al. (1990), is represented in Figure 1. The null discriminant curve, also displayed, separates focal, high vorticity, motions (above) from dissipative, high strain, motions (below). Focal motions are characterized by positive values of the second invariant, Q, while dissipative motions are associated with strong negative values of Q. Positive values of the third invariant, R, indicate two-dimensional extension with contraction in the third dimension, while R negative implies one-dimensional stretching with contraction in a plane.

Analogous quantities can be defined for the strain rate tensor, $S_{ij} = (A_{ij} + A_{ji})/2$ and its skew-symmetric part, $W_{ij} = (A_{ij} - A_{ji})/2$, the rate-of-rotation tensor. The nonzero second and third invariants of these tensors are R_S, Q_S and Q_W, defined as

$$Q_S = -\frac{1}{2} S_{ij} S_{ji} \quad (8)$$

$$R_S = -\frac{1}{3} S_{ij} S_{jk} S_{ki} \quad (9)$$

$$Q_W = -\frac{1}{2} W_{ij} W_{ji} \quad (10)$$

Q_S is always negative and is related to the kinetic energy dissipation rate ϵ, namely $\epsilon = -4\nu Q_S$. Q_W is always positive and is directly related to the square of the vorticity vector, often called enstrophy, by $Q_W = \omega^2/4$. The invariant R_S, apart from indicating the strength of the strain, characterizes its geometry: A positive R_S value implies two-dimensional extension with contraction in the third dimension, and negative R_S indicates the contrary.

RESULTS

The main objective of this work is to explore the correlations of the scalar molecular diffusion and the scalar dissipation with the velocity gradient invariants, in order to better understand the scalar mixing processes, and the role that the different velocity field coherent structures play in the scalar evolution. This has been done by calculating conditional averages for the four topologies described before, and obtaining Joint Probability Density Functions (JPDF) of scalar-related variables and velocity gradient invariants.

Data fields from 128^3 DNS runs with an inert scalar have been used to obtain the results presented in this work. From this data all the variables of interest defined previously can be calculated. The velocity field is forced and a Reynolds number $Re_\lambda \simeq 47$ is reached. This low Re_λ has been taken deliberately to ensure a proper numerical resolution in the second and third scalar derivatives. The initial scalar distribution is a double Dirac delta, taking the region in the center of the cube a scalar value $C = 1$ and the rest $C = 0$. The scalar mean is 0.5. The value of the Schmidt number, Sc, is 1.0. The results presented here correspond to a time when the scalar pdf has relaxed to a close-to-uniform distribution with two peaks near to the extreme values, 0 and 1.

The statistical calculations have been done from a total number of samples N=2,097,152 (= 128^3 mesh points in our simulation cube). The percentage of samples corresponding to each topology is 39.8 % for SF/S, 27.6 % for UF/C, 25.5 % for UN/S/S and 7.1 % for SN/S/S. While the scalar variance calculated for each of the four topologies results in the same value, the averaged scalar dissipation (0.1) in the UN/S/S samples is higher than the value obtained in SN/S/S (0.07), and about twice the values obtained for any of SF/S or UF/C samples (0.06 and 0.05). Similar behavior is found for the scalar diffusion rms.

Figure 2 displays $< D\nabla^2 c | c >$, the conditional diffusion of c, calculated for the different topologies detailed before. The molecular mixing appears clearly enhanced in UN/S/S regions and has a slightly weaker effect in the other topological structures. A functional dependence of the conditional diffusion on c can easily be proposed for each topology. Similar trends are observed for the scalar dissipation in Figure 3. $< \epsilon_c >$ reaches maximum values in UN/S/S structures, and has lower values in UF/C topologies.

The probability density functions obtained for the quantity $c_{,i}\, c_{,j}\, u_{j,i}$ in the four topologies are shown in Figure 4. All the curves are skewed towards negative values, which implies that the scalar dissipation production term in Eq. 5 has a positive average. This feature is enhanced in the strain dominated

topologies and the distribution corresponding to the UN/S/S topology presents a probability ten times higher respect to the others of large negative values. This indicates higher probability of strong scalar dissipation in strained regions, this effect being more intense in the case of planar strained structures of the flow.

The correlations of the scalar dissipation with $-Q_S$ (i.e. the strain) and with Q_W (i.e. the vorticity) can be observed in the joint pdfs depicted in Figures 5 and 6. The result for $-Q_S$ shows that the largest values of the scalar dissipation occur in the range of low and intermediate values of the kinetic energy dissipation ($-Q_S$), being the probability of high values of ϵ_c smaller as higher values of $-Q_S$ are considered. On the other hand, the largest values of ϵ_c appear for the smallest values of the enstrophy, as shown in Figure 6. The result which would indicate that scalar dissipation has little intensity in the core of high vorticity structures, generally filament shaped, and reaches significant values in the strained regions surrounding these vortex filaments.

Similar qualitative behavior is found for the joint statistics of the scalar diffusion with the vorticity and the strain. Figure 7 shows the JPDF of the diffusion term $D\nabla^2 c$ in Eq. 1 and $-Q_S$. The isocontours are symmetric, as expected, respect to the $-Q_S$ axis with the largest absolute values of the diffusion correlated with low and moderate strain magnitude. There is low probability of points with high strain and high diffusion values simultaneously. The JPDF of the scalar diffusion and $-Q_S$ is represented in Fig. 8. In this picture, the maximum absolute values of the diffusion are more probable to occur associated with minimum values of the vorticity, with the range of probability width for the scalar diffusion values decreasing uniformly as Q_W increases.

CONCLUSIONS

The mixing intensity depends on the velocity gradient invariants R and Q, i.e., on the character of the local motion pattern at each point in the flow, being the UN/S/S topology the one yielding the most efficient contribution to the scalar dissipation and to the scalar diffusion. From the results presented in this work, both processes are well correlated with low to moderate values of the strain and with minimum values of the vorticity. This behavior, at first sight surprising, can be physically interpreted: During the first stages of the scalar evolution, the mixing takes place whitin strong strain regions -associated with low vorticity values- with high efficiency. After a small time, the variance has been critically reduced and all the scalar is well mixed in those regions; therefore the diffusion and dissipation vanish there, but the mixing is still taking place in other regions with low to moderate strain magnitude. As the JPDFs presented here have been calculated after the initial scalar fields have relaxed, the significant correlations are found for these regions of low and moderate strain. Not a clear physical picture emerges from this description and further work is required to analise these issues. In order to complete the picture, more spatial information is desirable concerning the scalar dynamics whitin the coherent structures of the small scales such as the vorticity filaments, and the high strain regions. A final objective of this future research will be to parameterize the scalar mixing as a function of c, the Schmidt number, and some of the invariants R, Q, Q_S and Q_W.

ACKNOWLEDGEMENTS

The authors are grateful to the EU funding under the BRITE/EURAM Programme, Project BE95-1927.

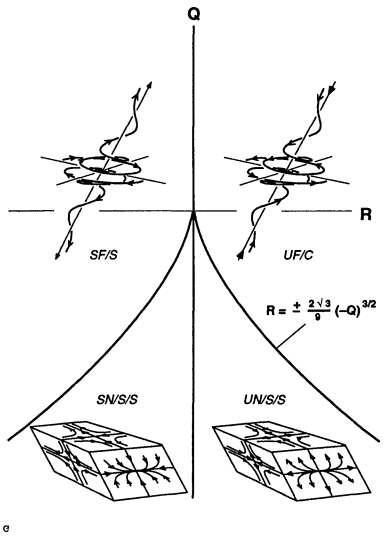

Fig. 1: Topological classification.

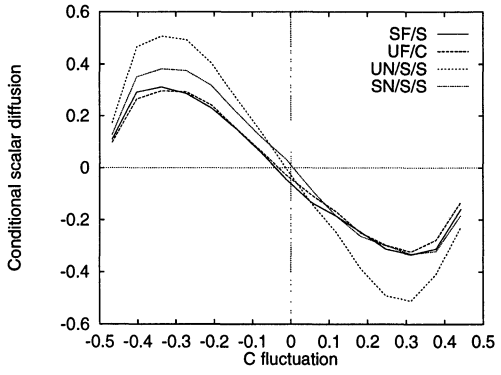

Fig. 2: Conditional scalar diffusion for the four topologies.

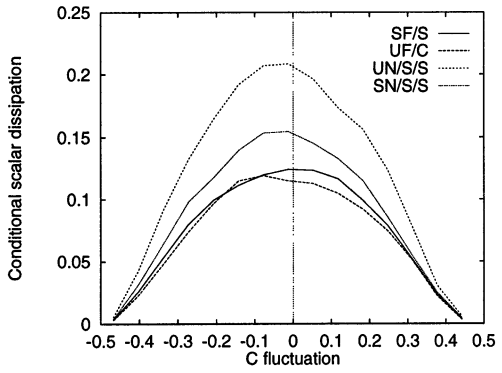

Fig. 3: Conditional scalar dissipation for the four topologies.

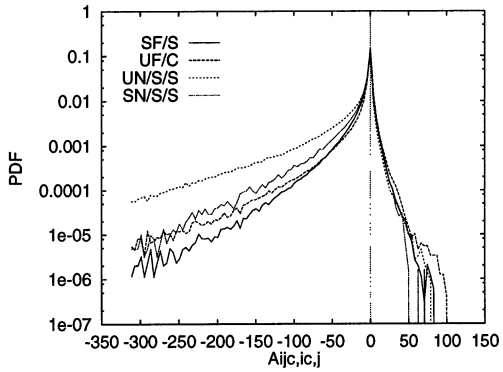

Fig. 4: pdf of the production term of scalar dissipation.

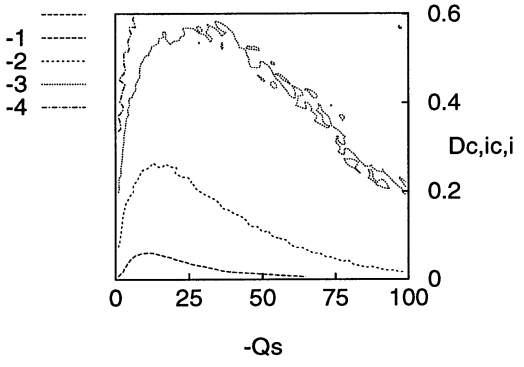

Fig. 5: Joint pdf of the invariant -Qs and the scalar dissipation.

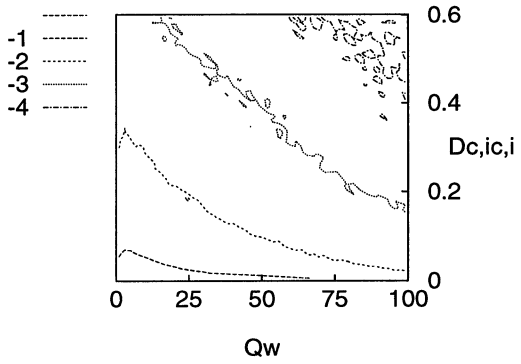

Fig. 6: Joint pdf of the invariant Qw and the scalar dissipation.

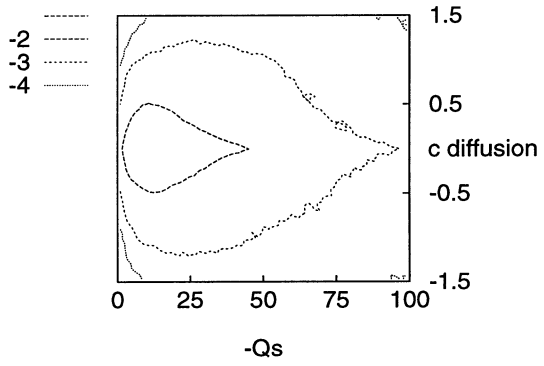

Fig. 7: Joint pdf of the invariant -Qs and the scalar diffusion.

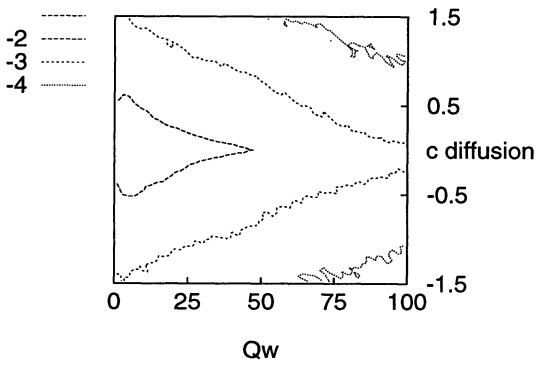

Fig. 8: Joint pdf of the invariant Qw and the scalar diffusion.

REFERENCES

Chong, M.S., Perry, A.E., and Cantwell, B.J. 1990. "A general classification of three-dimensional flow fields", *Phys. Fluids A*, **5**(2), 765-777.

Ottino, J. M. 1989. "The Kinematics of Mixing: Stretching, Chaos and Transport", Cambridge Univ. Press, N.Y.

Dopazo, C. 1994. "Recent Developments in PDF methods", In *Turbulent reacting flows*, Eds. Libby, P.A. and Williams, F.A., Ch 7, 375, Academic Press.

Kerr, R.M. 1985. "Higher-order derivative correlations and the alignment of small-scale structures in isotropic numerical turbulence", *J. Fluid Mech.* **153**(31).

Arhurst, W.T., Kerstein, A.R., Kerr, R.M., and Gibson, C.H. 1987. "Alignment of vorticity and scalar gradient with strain rate in simulated Navier-Stokes turbulence",*Phys. Fluids A*, **8**(30), 2343-2353.

Ruestch, G.R. and Maxey, M.R. 1991. "Small-scale features of vorticity and passive scalar fields in homogeneous isotropic turbulence", *Phys. Fluids A*, **3**(6), 1587-1597.

Pumir, A. 1994. "A numerical study of the mixing of a passive scalar in three dimensions in the presence of a mean gradient" *Phys. Fluids*, **6**(6), 2118-2132.